

Heisenberg machines with programmable spin-circuits

Saleh Bunaiyan^{1,3}, Supriyo Datta², and Kerem Y. Camsari³

¹*Electrical Engineering Department,*

*King Fahd University of Petroleum & Minerals (KFUPM),
Dhahran 31261, Saudi Arabia*

²*Elmore Family School of Electrical and Computer Engineering,
Purdue University, West Lafayette, Indiana 47907, USA and*

³*Department of Electrical and Computer Engineering,
University of California at Santa Barbara, Santa Barbara, CA 93106, USA*

(Dated: December 5, 2023)

We show that we can harness two recent experimental developments to build a compact hardware emulator for the classical Heisenberg model in statistical physics. The first is the demonstration of spin-diffusion lengths in excess of microns in graphene even at room temperature. The second is the demonstration of low barrier magnets (LBMs) whose magnetization can fluctuate rapidly even at sub-nanosecond rates. Using experimentally benchmarked circuit models, we show that an array of LBMs driven by an external current source has a steady-state distribution corresponding to a classical system with an energy function of the form $E = -1/2 \sum_{i,j} J_{ij} (\hat{m}_i \cdot \hat{m}_j)$. This may seem surprising for a non-equilibrium system but we show that it can be justified by a Lyapunov function corresponding to a system of coupled Landau-Lifshitz-Gilbert (LLG) equations. The Lyapunov function we construct describes LBMs interacting through the spin currents they inject into the spin neutral substrate. We suggest ways to tune the coupling coefficients J_{ij} so that it can be used as a hardware solver for optimization problems involving continuous variables represented by vector magnetizations, similar to the role of the Ising model in solving optimization problems with binary variables. Finally, we implement a Heisenberg AND gate based on a network of three coupled stochastic LLG equations, illustrating the concept of probabilistic computing with a programmable Heisenberg model.

With the slowing down of Moore’s law, there is tremendous interest in unconventional computing approaches. Prominent among these approaches are the energy-based models (EBMs) inspired by statistical physics, in which the problem is mapped to an energy function, such that the solution corresponds to the minimum energy state [1–3], which can then be identified using powerful optimization algorithms.

A particularly attractive way to find the minimum energy state of an energy function becomes possible if we can design a physical system whose natural physics makes it relax to this state. Such a system could be harnessed to solve this class of problems orders of magnitude faster and more efficiently than an algorithm implemented in software. An interesting EBM is the classical Heisenberg model

$$E = -\frac{1}{2} \sum_{i,j} J_{ij} (\hat{m}_i \cdot \hat{m}_j) \quad (1)$$

where $\hat{m}_{i,j}$ are unit vectors in 2D or 3D, which is different from the Ising model

$$E_{\text{ising}} = -\frac{1}{2} \sum_{i,j} J_{ij} s_i s_j \quad (2)$$

where s_i, s_j are variables with only two allowed values, ± 1 . Hopfield networks and Boltzmann machines based on the Ising model, Eq. (2), have generated tremendous recent excitement and even mapped to physical systems [4, 5]. The modern Hopfield network [6], based on the classical Heisenberg model, Eq. (1), shows promise in

machine learning applications and it should be of great interest to map it to an energy-efficient physical system.

In this letter, we propose and establish the feasibility of mapping Eq. (1) to a physical system consisting of an array of low barrier magnets (LBMs) interacting via spin currents through a spin-neutral channel (e.g., Cu, graphene) as shown in Fig. 1. The system is similar to the 2D graphene channels with long spin-diffusion length (λ_s) used to demonstrate room temperature spin logic [7–10], but with one *key difference*. Here, the magnets are not the usual stable magnets, but LBMs similar to those used to represent Ising spins or probabilistic bits (p-bits) [11, 12]. A charge current is driven through each LBM i by an external source, and the associated spin current diffuses through the substrate and exerts a spin-torque on a neighboring LBM j , leading to an effective interaction term J_{ij} between them.

Note that this is a particularly compact physical realization of Eq. (1) compared to the reported realizations of the Ising model (Eq. (2)) using p-bits [4, 13, 14], which require separate hardware to implement “synapses” that sense the state of each p-bit and drive neighboring p-bits accordingly. The structure proposed here (Fig. 1) integrates both the neuron and the synapse at once, thus making it possible to implement relatively fast synapses that can utilize the nanosecond fluctuations that have been demonstrated [15, 16] and could be designed to be even faster. The only additional hardware needed here is a final readout of the output magnets, rather than repeated readouts and re-injections from intermediate magnets.

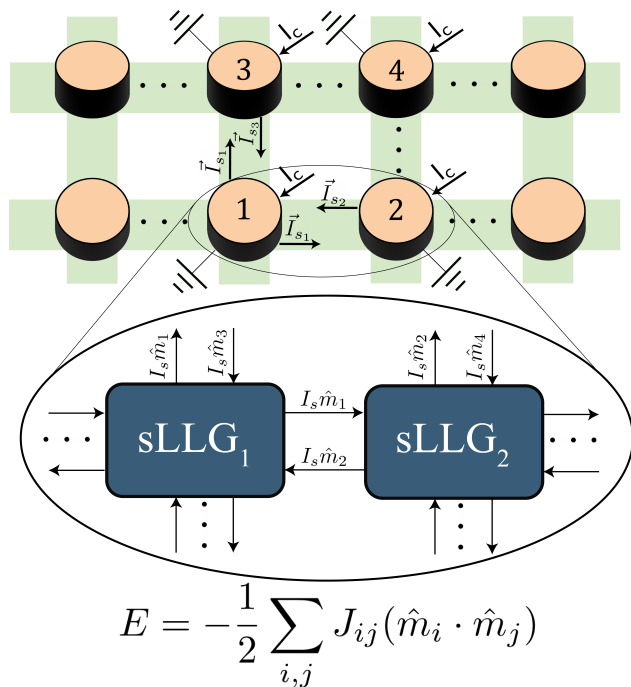


FIG. 1. **Heisenberg machines with programmable spin-circuits.** Low barrier magnets (LBMs) and the spin neutral channels form the Heisenberg array, where an external charge current is injected into the LBMs and thereby inducing a spin current inside the channel. Magnets are assumed to have a small energy barrier ($\Delta_B \rightarrow 0$) with no effective anisotropy ($\vec{H}_{\text{eff}} \rightarrow 0$). The proposed array is analogous to a system of coupled stochastic Landau–Lifshitz–Gilbert (sLLG) equations where each sLLG sends a spin current vector \vec{I}_s to its neighbors, where the spin current is defined as a function of the magnet magnetization $\vec{I}_{s_i} = I_s \hat{m}_i$. This coupled LBM system minimizes the Heisenberg Hamiltonian with continuous spin states, functioning as a Heisenberg machine, analogous to Ising machines.

The *central result* of this paper is to establish that the structure in Fig. 1 indeed minimizes a classical Heisenberg energy function of the form Eq. (1). This is not at all obvious since our structure is *not* at equilibrium and is not expected to necessarily obey a Boltzmann law $\propto \exp(-E/k_B T)$, $k_B T$, being the thermal energy. What we theoretically show is that an energy function of the form Eq. (1) constitutes a Lyapunov function that is minimized by the LBM dynamical equations. Our numerical simulations further indicate that different configurations also follow a Boltzmann law at least approximately.

Lyapunov functions.— To model a structure like Fig. 1 with N LBMs we start from a set of N coupled Landau–Lifshitz–Gilbert (LLG) equations using experimentally benchmarked physical parameters from [10, 17, 18], which were carefully derived from the work of Bauer, Brataas and Kelly on magnetoelectric circuit theory [19]. These were later turned into explicit circuit models that are modularly simulated in standard circuit simulators [17, 20, 21]. Throughout this letter, we focus on LBMs

with no shape or easy-plane anisotropy which can be practically built by reducing the energy barriers of magnets with perpendicular anisotropy (PMA). To illustrate the Lyapunov function approach, we first show that a single magnet (\hat{m}_1) with an injected spin current \vec{I}_s , coming from another fixed magnet \hat{m}_2 such that $\vec{I}_s = I_s \hat{m}_2$, minimizes the function

$$E = - \left(\frac{I_s}{I_0} \right) \hat{m}_1 \cdot \hat{m}_2 = -J_{12} \hat{m}_1 \cdot \hat{m}_2 \quad (3)$$

where J_{12} is the dimensionless and symmetric coupling ($J_{12} = J_{21}$) coefficient defined as I_s/I_0 . I_0 is a constant given by $2q\alpha k_B T/\hbar$ where q is the electron charge, \hbar is the reduced Planck’s constant and α is the damping coefficient of the nanomagnet. I_0 can be formally derived from the Fokker-Planck equation (FPE) [22] as we show in the supplementary. We show that dE/dt is always negative by starting from the deterministic LLG equation [23, 24] for \hat{m}_1 :

$$(1 + \alpha^2) \frac{d\hat{m}_1}{dt} = \frac{\hat{m}_1 \times \vec{I}_s \times \hat{m}_1}{qN_s} + \frac{\alpha(\hat{m}_1 \times \vec{I}_s)}{qN_s} \quad (4)$$

where N_s being the total number of spins in magnet 1.

We then extend this result to a system of N coupled LBMs, described by N coupled LLG equations (see supplementary):

$$(1 + \alpha^2) \frac{d\hat{m}_i}{dt} = \frac{\hat{m}_i \times I_0 \vec{I}_i \times \hat{m}_i}{qN_s} + \frac{\alpha(\hat{m}_i \times I_0 \vec{I}_i)}{qN_s} \quad (5)$$

with $\vec{I}_i = \sum_j J_{ij} \hat{m}_j$, assuming the interaction strength to be symmetric ($J_{ij} = J_{ji}$). These equations imply $dE/dt \leq 0$, where E is now the classical Heisenberg model described in Eq. (1). As a result, the system dynamics always tend to minimize a classical Heisenberg model whose parameters J_{ij} can be programmed. This description of a non-equilibrium system with an equilibrium model is reminiscent of spin-currents interacting with PMA magnets [25].

Numerical simulation.— We will now present numerical results for two examples: a system of two LBMs and a frustrated system of three LBMs, indicating that the results not only minimize the Lyapunov function in Eq. (1), but also follow the Boltzmann law, where states are sampled according to $\rho(\hat{m}_1, \hat{m}_2, \dots, \hat{m}_N) \propto \exp[-E(\hat{m}_1, \hat{m}_2, \dots, \hat{m}_N)]$.

The physical structure of the two studied systems are described in Figs. 2(a) and 2(d). All magnets were chosen to be identical and receive the same input current I_c . In our setup, the charge current I_c flows to a nearby ground injecting pure spin-currents in all directions, as commonly done in non-local spin valves [10, 26]. Simulations were carried out on a standard circuit simulator (HSPICE) using 4-component spin-circuits [17, 27]. The full circuits used for simulating the two examples are shown in Figs. 2(b) and 2(e). The used modules are of two categories: transport and magnetism, where the

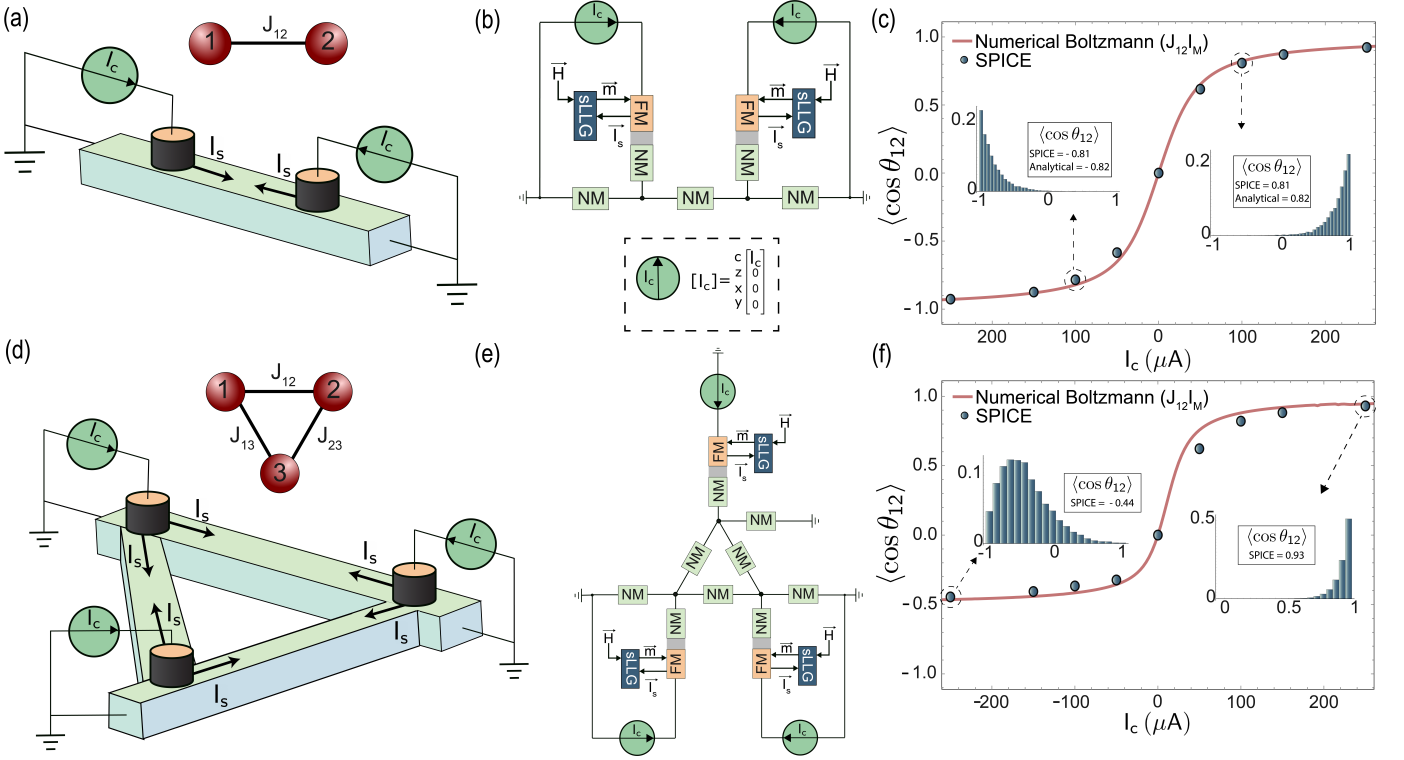


FIG. 2. **Simulated hardware for the Heisenberg emulator.** (a) 2-LBM system that emulates a Heisenberg model of two spins. (b) Simulated configuration in HSPICE using benchmarked circuit models. Transport physics from the LBM to the channel and from the channel to the ground are characterized by an FM|NM and NM modules, respectively. Magnetization dynamics of the LBM are described by the sLLG modules. All circuits are described by 4 components: charge, and spins (z, x, y). (c) The Boltzmann solution is related to the proposed hardware through I_M that takes the charge-to-spin conversions into account. The relation between spin current and interaction strength is given by ($J_{12} = I_s/I_0$). (d) 3-LBM system that emulates a Heisenberg model of three spins in a frustrated configuration. (e) Simulated configuration in HSPICE. (f) Boltzmann solution for the 3-magnet system. We use the same I_M value in the 2-magnet system (even though a new charge-to-spin mapping may need to be measured or calculated, see supplementary). Insets show the probability distribution of the magnets correlation $\cos \theta_{12}$ at a given input I_c , which can be analytically derived for two LBMs (see supplementary).

transport through LBMs into the spin-neutral channel are characterized by an FM|NM interface module, which defines the interface between the ferromagnet (FM) and the normal metal (NM) [17, 19]. The magnetic fluctuations of LBMs are described by the stochastic LLG (sLLG) module, carefully benchmarked against corresponding FPEs for monodomain magnets [25, 27]. The spin-neutral channel between LBMs is solely described by the transport module NM. All transport modules are represented by 4×4 matrices describing the interactions between charge and spins in the z, x, y directions. The physical parameters we used are reported in the supplementary.

The correlation between the two coupled LBMs can be described by the cosine of the relative angle between their magnetization vectors $\langle \cos \theta_{12} \rangle$. If the two LBMs are coupled by a J_{ij} , their correlation can be computed from a Boltzmann-like equation using Eq. (1):

$$\langle \cos \theta_{12} \rangle = \int_{S_1} \int_{S_2} \frac{1}{Z} \cos \theta_{12} \exp(-E) dS_1 dS_2 \quad (6)$$

where ($dS_i = \sin(\theta_i) d\theta_i d\phi_i$) describes integration on the surface of the unit sphere and Z is the partition function. For any given symmetric coupling J_{ij} between LBM 1 and 2, we can evaluate Eq. (6) numerically. To make contact between the circuit shown in Fig. 2(a) and Eq. (6) however we need a normalizing parameter such that $J_{ij} = I_{sij}/I_0$ where I_{sij} is the component of the spin-current along magnet j incident to magnet i . We need another configuration-dependent parameter relating the injected charge current to the spin-currents. We define a single parameter, I_M that combines the two such that $J_{ij} = (I_c/I_M)$. For the 2-magnet system, we can find I_{sij} analytically by defining a new basis: ($\hat{m}_1, \hat{m}_2, \hat{m}_1 \times \hat{m}_2$) similar to the approach used in [28]. By a clever coordinate transformation, we exactly solve for I_M in the 2-magnet system in the supplementary. Numerical results from our spin-circuits match those obtained from our analytical solution, as shown in FIG. 2. Note that in general systems ($N > 2$), I_M may depend on the geometry of the channel and it may need to be found by experimental calibration in different systems.

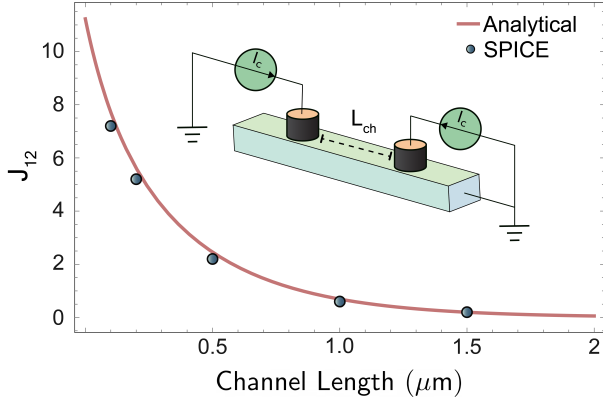


FIG. 3. **Programmability of the interaction strength** J_{ij} . At fixed charge current I_c , the NM channel between LBMs encodes the magnitude of the coupling strength between magnets. Extending the channel length L_{ch} reduces the correlation between the magnets due to more spins being neutralized. The polarity of the J_{ij} is controlled through the direction of the input current I_c . The analytical analysis is provided in the supplementary, we assume the channel to be Cu with 400 nm spin-diffusion length.

We then study a frustrated system of three magnets, with the emulation hardware shown in Fig. 2(d), described by the Boltzmann law as:

$$\langle \cos \theta_{12} \rangle = \int_{S_1} \int_{S_2} \int_{S_3} \frac{1}{Z} \cos \theta_{12} \exp(-E) dS_1 dS_2 dS_3 \quad (7)$$

All magnets have identical charge inputs (swept from negative to positive values of I_c where positive electron current is measured from the magnet into the channel) leading to a uniform $J_{ij} = \pm J_0$, ferromagnetic/antiferromagnetic interactions. At all currents we observe identical correlations, *i.e.*, $\langle \theta_{12} \rangle = \langle \theta_{13} \rangle = \langle \theta_{23} \rangle$, and thus we only report $\langle \cos \theta_{12} \rangle$ without loss of generality in Fig. 2. Similar to the 2-magnet system, positive currents lead to ferromagnetic correlation, however, negative currents result in a saturated correlation of $\cos \theta_{12} = -0.5$ where each magnet (on average) has a maximum of 120 degree separation between its neighbors (Fig. 2(f)), reminiscent of frustrated magnets realizing XY models [2].

Power estimation.—Since the proposed hardware comprises both the neuron and the synapse, the power consumption is expected to be order of magnitude less than possible digital implementations. There are no detailed estimations of the digital footprint for continuous stochastic neurons, however, transistor-level projections indicate that tens of thousands of transistors operating at 10's of μW 's are needed even for *binary* stochastic neurons [29, 30]. To generate significant correlations, our systems presented in Fig. 2 consumes around 180 nW and 270 nW for the 2-LBM and the 3-LBM systems, about 100 nW per LBM terminal. We measure this power as the average at the two extremes of input charge currents for the ferromagnetic and the anti-ferromagnetic cases.

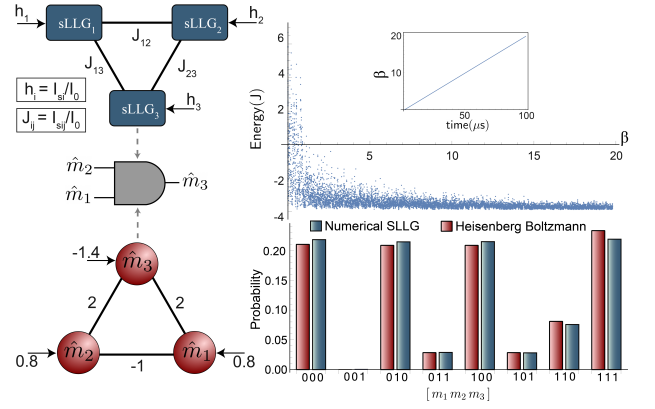


FIG. 4. **Heisenberg AND Gate.** Programming three coupled LBMs modeled by sLLGs. The interaction strength $J_{ij} = I_{sij}/I_0$ and bias terms $h_i = I_{si}/I_0$ (shown in the figure) are chosen to implement a Heisenberg AND gate, continuous spins were binarized by thresholding at zero. The network was annealed with a linear profile of β (scaling the weights). Results show saturation around the ground state of the network. The truth table of the AND was verified numerically by the network response, matching the expected response obtained by the Boltzmann law. For the histogram producing the truth table, the network was simulated at a constant $\beta = 4$.

These numbers can be understood by relating the necessary spin-currents to charge currents. Spin-currents need to be around $\approx \pm 15 I_0 \approx 1.88 \mu\text{A}$ to create large negative or positive correlations. With interface polarizations of $P \approx 0.1$, interface and side channel resistances of $R_{int} \approx 1 \Omega$, $R_{side} \approx 0.5 \Omega$, a spin-diffusion length of 400 nm along 200 nm channels, and resistive division factors diverting the spin-currents, charge currents of around $I_c = 250 \mu\text{A}$ are needed (see supplementary). These charge currents lead to $I_c^2 R$ losses of around 100 nW per LBM arm. Considering the 10-20 μW estimations for *binary* stochastic neurons for the simpler *Ising* model, the proposed emulator should be at least 3 to 4 orders of magnitude more energy-efficient over digital implementations of the classical Heisenberg model.

Programmability.—Another practical aspect is the tunability of the interaction strengths, J_{ij} . In the proposed hardware, these interactions are described by the amount of spin current received from the other LBMs, which can be tuned through many parameters (e.g., input current, channel material, etc.). In Fig. 3, we analyze the programmability of J_{ij} for a channel by tuning the channel length L_{ch} , the spin-diffusion length for Cu is around 400 nm at room temperature [31], results show a reasonable tunability range for J_{ij} . Recently, it was reported that graphene can have a spin-diffusion length of up to 26 μm at room temperature [9]. Having longer spin-diffusion length relaxes the constraints on tuning the interaction strength J_{ij} and we can achieve higher values of J_{ij} , both are critical for machine learning applications, such as Boltzmann Machines [32, 33]. Throughout, we assumed configurations where all charge currents have the same

sign and magnitude, leading to J_{ij} with the same sign. However, systems with frustration involves positive and negative J_{ij} . In the supplementary, we discuss how to do $\pm J_{ij}$ in one configuration using auxiliary magnets.

Readout of LBMs.—An important practical consideration is the ability to read out the correlations induced in LBMs. Advances in modern spintronic capabilities offer various possibilities. We briefly consider three approaches that could be used. First, an experimentally demonstrated approach is using nearby ferromagnets for potentiometric read out, e.g., as commonly used for topological insulators (TI) [34, 35]. Secondly, inverse spin Hall effects in heavy metals and TIs can be used via terminals placed near the LBMs [36, 37]. Finally, magnetic tunnel junctions built on top of the LBMs could be used for read-out as commonly used in spin-orbit torque-based structures [38]. This approach may require isolated and separate terminals for the MTJ-read out and the charge injection over the LBM similar to those in all-spin logic devices and potentially is more challenging from a fabrication point of view [39].

Computation with Heisenberg models.—Next, we show a Heisenberg AND gate based on three coupled sLLG equations as shown in Fig. 4, without our full transport modules. By changing the interaction coefficients by linearly scaling the weights through β , we anneal the system. In practice, this could be done, for example, by increasing the charge current injected into the LBMs. Our annealing result aligns well with the ground state, the error in the network minimum state is around 0.03% after 100 μ s. We also obtain the full truth table for the AND gate by observing the network output at fixed β for 400 μ s. To generate Boolean output values, continuous spins were binarized using thresholding at the zero point. No thresholding was performed during the simulation; all spins were binarized post-simulation. Figure 4 shows that the network response is identical to that one obtained by the Boltzmann law, and in agreement with

probabilistic AND gate operation. Further details are provided in supplementary. In this example, we showed the invertible logic operation of a probabilistic AND gate with *Boolean* output states, however, the continuous nature of our spins could also be useful in the areas of stochastic computing where arithmetic operations such as multiplication, division and factorization can be simplified by continuous stochastic neurons [40].

This letter presented compact LBM spin-circuits emulating the classical Heisenberg model. We established the equivalence between spin-circuits and the classical Heisenberg model analytically and numerically. With tremendous interest in building programmable physics-inspired computing hardware for the *Ising* model, the compact and energy-efficient realization of the classical Heisenberg model could be useful for a number of applications from training modern Hopfield networks to solving continuous optimization problems. We leave natural extensions of the concept to in-plane magnetic anisotropy (IMA) magnets realizing the classical XY model for future investigation. We envision that spin-circuit networks with LBMs can be extended beyond conservative systems described by an energy, such as Bayesian (Belief) networks with asymmetric network connections [33, 41, 42].

The spin-circuit codes used in this study are publicly available on GitHub [43].

ACKNOWLEDGMENT

We acknowledge support from ONR-MURI grant N000142312708, OptNet: Optimization with p-Bit Networks. The authors are grateful to Shun Kanai, Saroj Dash, Punyashloka Debashis and Zhihong Chen for fruitful discussions.

-
- [1] Y. W. Teh, M. Welling, S. Osindero, and G. E. Hinton, *Journal of Machine Learning Research* **4**, 1235 (2003).
 - [2] N. G. Berloff, M. Silva, K. Kalinin, A. Askitopoulos, J. D. Töpfer, P. Cilibrizzi, W. Langbein, and P. G. Lagoudakis, *Nature Materials* **16**, 1120 (2017).
 - [3] P. Huembeli, J. M. Arrazola, N. Killoran, M. Mohseni, and P. Wittek, *Quantum Machine Intelligence* **4**, 10.1007/s42484-021-00057-7 (2022).
 - [4] W. A. Borders, A. Z. Pervaiz, S. Fukami, K. Y. Camsari, H. Ohno, and S. Datta, *Nature* **573**, 390 (2019).
 - [5] N. Mohseni, P. L. McMahon, and T. Byrnes, *Nature Reviews Physics* **4**, 363 (2022).
 - [6] H. Ramsauer, B. Schäfl, J. Lehner, P. Seidl, M. Widrich, T. Adler, L. Gruber, M. Holzleitner, M. Pavlović, G. K. Sandve, V. Greiff, D. Kreil, M. Kopp, G. Klambauer, J. Brandstetter, and S. Hochreiter, *Hopfield networks is all you need* (2021), arXiv:2008.02217.
 - [7] R. Ishihara, Y. Ando, S. Lee, R. Ohshima, M. Goto, S. Miwa, Y. Suzuki, H. Koike, and M. Shiraishi, *Phys. Rev. Appl.* **13**, 044010 (2020).
 - [8] J. Panda, M. Ramu, O. Karis, T. Sarkar, and M. V. Kamalakar, *ACS Nano* **14**, 12771 (2020).
 - [9] T. Bisswanger, Z. Winter, A. Schmidt, F. Volmer, K. Watanabe, T. Taniguchi, C. Stampfer, and B. Beschoten, *Nano Letters* **22**, 4949 (2022).
 - [10] D. Khokhriakov, S. Sayed, A. M. Hoque, B. Karpiak, B. Zhao, S. Datta, and S. P. Dash, *Phys. Rev. Appl.* **18**, 064063 (2022).
 - [11] K. Y. Camsari, R. Faria, B. M. Sutton, and S. Datta, *Physical Review X* **7**, 031014 (2017).
 - [12] K. Y. Camsari, S. Salahuddin, and S. Datta, *IEEE Electron Device Letters* **38**, 1767 (2017).
 - [13] J. Kaiser, W. A. Borders, K. Y. Camsari, S. Fukami, H. Ohno, and S. Datta, *Phys. Rev. Appl.* **17**, 014016 (2022).

- [14] A. Grimaldi, K. Selcuk, N. A. Aadit, K. Kobayashi, Q. Cao, S. Chowdhury, G. Finocchio, S. Kanai, H. Ohno, S. Fukami, and K. Y. Camsari, in *2022 International Electron Devices Meeting (IEDM)* (2022) pp. 22.4.1–22.4.4.
- [15] K. Hayakawa, S. Kanai, T. Funatsu, J. Igarashi, B. Jinnai, W. A. Borders, H. Ohno, and S. Fukami, *Phys. Rev. Lett.* **126**, 117202 (2021).
- [16] C. Safranski, J. Kaiser, P. Trouilloud, P. Hashemi, G. Hu, and J. Z. Sun, *Nano Letters* **21**, 2040 (2021).
- [17] K. Y. Camsari, S. Ganguly, and S. Datta, *Scientific Reports* **5**, 10.1038/srep10571 (2015).
- [18] S. Sayed, V. Q. Diep, K. Y. Camsari, and S. Datta, *Scientific Reports* **6**, 10.1038/srep28868 (2016).
- [19] A. Brataas, G. E. Bauer, and P. J. Kelly, *Physics Reports* **427**, 157 (2006).
- [20] S. Srinivasan, V. Diep, B. Behin-Aein, A. Sarkar, and S. Datta, Modeling multi-magnet networks interacting via spin currents, in *Handbook of Spintronics*, edited by Y. Xu, D. Awschalom, and J. Nitta (Springer Netherlands, 2016) pp. 1281–1335.
- [21] S. Manipatruni, D. E. Nikonov, and I. A. Young, *IEEE Transactions on Circuits and Systems I: Regular Papers* **59**, 2801 (2012).
- [22] W. F. Brown Jr, *Physical review* **130**, 1677 (1963).
- [23] J. Z. Sun, *Physical Review B* **62**, 570 (2000).
- [24] J. Z. Sun, T. Kuan, J. Katine, and R. H. Koch, in *Quantum Sensing and Nanophotonic Devices*, Vol. 5359 (SPIE, 2004) pp. 445–455.
- [25] W. H. Butler, T. Mewes, C. K. A. Mewes, P. B. Visscher, W. H. Rippard, S. E. Russek, and R. Heindl, *IEEE Transactions on Magnetics* **48**, 4684 (2012).
- [26] T. Kimura, Y. Otani, and J. Hamrle, *Physical review letters* **96**, 037201 (2006).
- [27] M. M. Torunbalci, P. Upadhyaya, S. A. Bhave, and K. Y. Camsari, *IEEE Transactions on Electron Devices* **65**, 4628 (2018).
- [28] D. Datta, B. Behin-Aein, S. Datta, and S. Salahuddin, *IEEE Transactions on Nanotechnology* **11**, 261 (2011).
- [29] K. Kobayashi, N. Singh, Q. Cao, K. Selcuk, T. Hu, S. Niaz, N. A. Aadit, S. Kanai, H. Ohno, S. Fukami, *et al.*, arXiv preprint arXiv:2304.05949 (2023).
- [30] P. Debashis, H. Li, D. Nikonov, and I. Young, *IEEE Magnetics Letters* **13**, 1 (2022).
- [31] T. Kimura, T. Sato, and Y. Otani, *Phys. Rev. Lett.* **100**, 066602 (2008).
- [32] G. E. Hinton, T. J. Sejnowski, and D. H. Ackley, *Boltzmann Machines: Constraint Satisfaction Networks That Learn*, Tech. Rep. CMU-CS-84-119, (Computer Science Department, Carnegie Mellon University, 1984).
- [33] D. H. Ackley, G. E. Hinton, and T. J. Sejnowski, *Cognitive Science* **9**, 147 (1985).
- [34] S. Hong, V. Diep, S. Datta, and Y. P. Chen, *Physical Review B* **86**, 085131 (2012).
- [35] J. Kim, C. Jang, X. Wang, J. Paglione, S. Hong, J. Lee, H. Choi, and D. Kim, *Physical Review B* **99**, 245148 (2019).
- [36] W. Y. Choi, I. C. Arango, V. T. Pham, D. C. Vaz, H. Yang, I. Groen, C.-C. Lin, E. S. Kabir, K. Oguz, P. Debashis, *et al.*, *Nano Letters* **22**, 7992 (2022).
- [37] V. T. Pham, I. Groen, S. Manipatruni, W. Y. Choi, D. E. Nikonov, E. Sagasta, C.-C. Lin, T. A. Gosavi, A. Marty, L. E. Hueso, *et al.*, *Nature Electronics* **3**, 309 (2020).
- [38] L. Liu, C.-F. Pai, Y. Li, H. Tseng, D. Ralph, and R. Buhrman, *Science* **336**, 555 (2012).
- [39] B. Behin-Aein, D. Datta, S. Salahuddin, and S. Datta, *Nature nanotechnology* **5**, 266 (2010).
- [40] A. Alaghi and J. P. Hayes, *ACM Transactions on Embedded computing systems (TECS)* **12**, 1 (2013).
- [41] K.-E. Harabi, T. Hirtzlin, C. Turck, E. Vianello, R. Laurent, J. Droulez, P. Bessière, J.-M. Portal, M. Bocquet, and D. Querlioz, *Nature Electronics* 10.1038/s41928-022-00886-9 (2022).
- [42] P. Debashis, V. Ostwal, R. Faria, S. Datta, J. Appenzeller, and Z. Chen, *Scientific Reports* **10**, 10.1038/s41598-020-72842-6 (2020).
- [43] S. Bunaiyan and K. Y. Camsari, Heisenberg machines (HSPICE code), <https://github.com/OPUSLab/HeisenbergMachines> (2023).

Supplementary Material

I. FOKKER-PLANCK EQUATION FOR COUPLED LBMS

Consider a single low-barrier ($\Delta_B \rightarrow 0$) magnet \hat{m}_1 with no effective anisotropy ($\vec{H}_{\text{eff}} = 0$) that is under the influence of a spin current, \vec{I}_s incident to it. Suppose \vec{I}_s is polarized in the direction of another fixed magnet, \hat{m}_2 , such that $\vec{I}_s = I_s \hat{m}_2$. We will assume $\hat{m}_2 = \hat{z}$ without loss of generality. For this system, the following Fokker Planck equation (FPE) can be written at steady-state [22]:

$$\left(\frac{\alpha \gamma k_B T}{(1 + \alpha^2) M_s \text{Vol.}} \right) \nabla^2 P(\theta_1, \phi_1) - \nabla \cdot \left(P(\theta_1, \phi_1) \frac{d\hat{m}_1}{dt} \right) = 0 \quad (\text{S.1})$$

where α is the damping coefficient, γ is the gyromagnetic ratio of the electron, M_s is the saturation magnetization of the magnet, Vol. is the volume of the magnetic body, $k_B T$ is the thermal energy and $P(\theta_1, \phi_1)$ is the probability density function for the magnetization, \hat{m}_1 . In turn, $d\hat{m}_1/dt$ can be obtained from the Landau-Lifshitz-Gilbert (LLG) equation:

$$(1 + \alpha^2) \frac{d\hat{m}_1}{dt} = \frac{\hat{m}_1 \times \vec{I}_s \times \hat{m}_1}{qN_s} + \frac{\alpha(\hat{m}_1 \times \vec{I}_s)}{qN_s} \quad (\text{S.2})$$

where q is the electron charge and N_s is the number of spins in the magnetic volume, *i.e.*, $N_s = M_s \text{Vol.} / \mu_B$, μ_B being the Bohr magneton. We can then write down the solution:

$$P(\theta_1, \phi_1) = \frac{1}{Z} \exp\left(\hat{m}_1 \cdot \frac{\vec{I}_s}{I_0}\right) \quad (\text{S.3})$$

where we defined

$$I_0 = \frac{2q\alpha k_B T}{\hbar} \quad (\text{S.4})$$

Direct substitution of Eq. (S.3) into Eq. (S.1) shows, after several steps of tedious algebra, the solution satisfies the Fokker-Planck equation. The form of Eq. (S.3) allows us to define a dimensionless energy for this non-equilibrium system, such that:

$$E = -\left(\frac{I_s}{I_0}\right) \hat{m}_1 \cdot \hat{m}_2 \quad (\text{S.5})$$

where the steady-state probability of the system follows a Boltzmann-like law, with

$$P(\theta_1, \phi_1) = \frac{1}{Z} \exp(-E) \quad (\text{S.6})$$

II. LYAPUNOV FUNCTIONS

Armed with our result in Eq. (S.5), we consider Lyapunov functions for $N = 2$ and $N > 2$ magnet systems. The main idea is to find an “energy” whose rate of change is nonnegative:

$$\frac{dE}{dt} = \vec{\nabla}_{\hat{m}} E \cdot \frac{d\hat{m}}{dt} \leq 0 \quad (\text{S.7})$$

Here we will prove that an energy of the form of Eq. (S.5) satisfies the above condition which we will extend to systems of magnets, $N > 2$.

Two magnet system: Consider the same scenario we started from in Eq. (S.1): magnet \hat{m}_1 is receiving a spin current, \vec{I}_s , polarized in the direction of another fixed magnet, \hat{m}_2 , such that $\vec{I}_s = I_s \hat{m}_2 = (I_0) J_{12} \hat{m}_2$, where I_0 is defined in Eq. (S.4). J_{12} is the dimensionless coupling between magnet 2 and magnet 1. For this system, define the Lyapunov function, E , as:

$$E = -\left(\frac{I_s}{I_0}\right) \hat{m}_1 \cdot \hat{m}_2 \quad \text{with} \quad \vec{\nabla}_{\hat{m}_1} E = -\left(\frac{I_s}{I_0}\right) \hat{m}_2 = -\frac{\vec{I}_s}{I_0} \quad (\text{S.8})$$

From the LLG equation for \hat{m}_1 (Eq. (S.2)), we obtain:

$$C \frac{d\hat{m}_1}{dt} = \vec{I}_s - \hat{m}_1 (\hat{m}_1 \cdot \vec{I}_s) + \alpha (\hat{m}_1 \times \vec{I}_s) \quad (\text{S.9})$$

where we defined $C = qN_s(1 + \alpha^2) > 0$. Combinations of Eq. (S.9) and Eq. (S.8) using Eq. (S.7) yields:

$$C \frac{dE}{dt} = -\frac{\vec{I}_s}{I_0} \cdot [\vec{I}_s - \hat{m}_1 (\hat{m}_1 \cdot \vec{I}_s) + \alpha (\hat{m}_1 \times \vec{I}_s)] \quad (\text{S.10})$$

Finally by simplifying Eq. (S.10) we can show that the condition for energy minimization is satisfied:

$$C \frac{dE}{dt} = -\frac{[\vec{I}_s \cdot \vec{I}_s - (\hat{m}_1 \cdot \vec{I}_s)^2]}{I_0} \leq 0 \quad (\text{S.11})$$

N -magnet system: Given how the Lyapunov function for the 2-magnet system can be formally derived to follow a Boltzmann-like equation, we posit the following Lyapunov function for the N -magnet system:

$$E = -\frac{1}{2} \sum_{i,j} J_{ij} (\hat{m}_i \cdot \hat{m}_j) = -\frac{1}{2} \sum_{i,j} \frac{I_{sij}}{I_0} (\hat{m}_i \cdot \hat{m}_j) \quad (\text{S.12})$$

The input to the i^{th} magnet could be defined as $\vec{I}_i = \sum_j J_{ij} \hat{m}_j$. Assuming the reciprocity of the interaction strengths ($J_{ij} = J_{ji}$):

$$\vec{\nabla}_{\hat{m}_i} E = - \sum_j J_{ij} \hat{m}_j = -\vec{I}_i \quad (\text{S.13})$$

The coupled LLG equations for N -magnets can be written as:

$$C \frac{d\hat{m}_i}{dt} = I_0 [\vec{I}_i - \hat{m}_i (\hat{m}_i \cdot \vec{I}_i) + \alpha (\hat{m}_i \times \vec{I}_i)] \quad (\text{S.14})$$

Combinations of Eq. (S.14) and Eq. (S.13) with equation (S.7) yields:

$$C \frac{dE}{dt} = \sum_i -(\vec{I}_i \cdot I_0 [\vec{I}_i - \hat{m}_i (\hat{m}_i \cdot \vec{I}_i) + \alpha (\hat{m}_i \times \vec{I}_i)]) \quad (\text{S.15})$$

by noting that ($\sum_i \vec{I}_i \cdot \alpha (\hat{m}_i \times \vec{I}_i) = 0$), the expression can be further simplified to:

$$C \frac{dE}{dt} = \sum_i -I_0 [\vec{I}_i \cdot \vec{I}_i - (\hat{m}_i \cdot \vec{I}_i)^2] \leq 0 \quad (\text{S.16})$$

which shows that the condition for energy minimization is also satisfied for N -magnets.

III. LANGEVIN FUNCTION

From our results in Eq. (S.3) we can obtain the average magnetization $\langle m_z \rangle$ for a single magnet:

$$\langle m_z \rangle = \frac{\int_{\theta=0}^{\theta=\pi} \int_{\phi=0}^{\phi=2\pi} \cos(\theta) / Z \exp\left(\frac{I_s}{I_0} \cos(\theta)\right) \sin(\theta) d\theta d\phi}{\int_{\theta=0}^{\theta=\pi} \int_{\phi=0}^{\phi=2\pi} 1 / Z \exp\left(\frac{I_s}{I_0} \cos(\theta)\right) \sin(\theta) d\theta d\phi} \quad (\text{S.17})$$

which is found to be the Langevin function:

$$\langle m_z \rangle = \langle \cos \theta \rangle = \coth\left(\frac{I_s}{I_0}\right) - \frac{I_0}{I_s} \quad (\text{S.18})$$

where $I_0 = \frac{2q}{\hbar} k_B T \alpha$ as defined previously.

The Langevin function exactly overlaps with the Boltzmann numerical solution of $\langle \cos \theta_{12} \rangle$ shown in Fig. S.1(b). The overlap was confirmed through numerical solution and it reproduced our results from SPICE simulations as shown in the insets of Fig. 2.

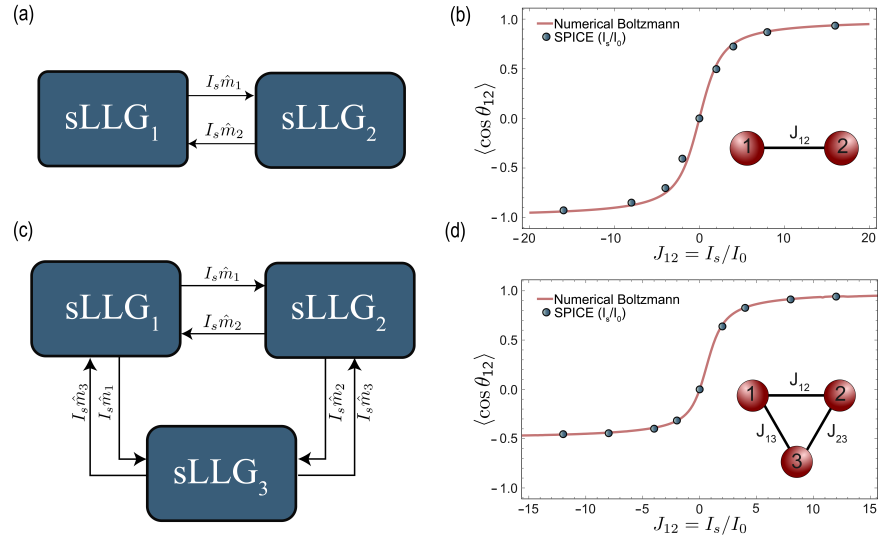


FIG. S.1. Coupled LBMs with pure spin currents. (a) Two coupled sLLG equations, where each sLLG sends a spin current along its magnetization direction $\vec{I}_{s_i} = I_s \hat{m}_i$ to the other sLLG. (b) The two coupled sLLG equations are contacted to the Boltzmann numerical solution by the predefined constant I_0 . (c) Three coupled sLLG equations in a frustrated configuration. (d) The three coupled sLLG equations also match with the Boltzmann law, note that I_0 is configuration independent.

IV. COUPLED LBMS WITHOUT TRANSPORT

In Fig. S.1, we compute correlations purely based on *spin-currents* without any transport physics that involve conversions from charge currents to spin-currents. We consider coupled sLLG equations for two and three magnet systems and compute correlations between the magnets. We then compare these correlations with numerically obtained Boltzmann probabilities ($\rho = Z^{-1} \exp(-E)$) using the dimensionless energy of the form

$$E = - \sum_{i,j} J_{ij} (\hat{m}_i \cdot \hat{m}_j) \quad (\text{S.19})$$

where $J_{ij} = (I_{s_{ij}}/I_0)$. Our numerical results indicate that the two and three magnet systems are well-described by this approach, indicating the generality of the constant I_0 . In the case of 2-magnets, correlations obtained from the numerical Boltzmann approach amounts to taking the Langevin function as a function of I_s . We note that the results shown in the main text, Fig. 2 show deviations because the transport parameters relating charge currents to spin currents turn out to be different in different systems. These purely spin-current based results may suggest alternative physical realizations of coupled LBMs without involving charge currents.

V. SPIN-CIRCUIT MODULES

Spin-circuits [17, 19–21] provide a generalization of ordinary charge circuits where each node in the circuit is represented by a 4-dimensional voltage, $([V_c V_z V_x V_y]^T)$ corresponding to 3-spin components (z, x, y) and 1-charge component. Fig. S.2 shows the details of the spin-circuit for the 2-LBM system considered in the main paper. For the normal metal (NM) module, the series conductance G_{se} and the shunt conductance G_{sh} are defined as:

$$G_{se} = \begin{bmatrix} c & z & x & y \\ c & G_c & 0 & 0 & 0 \\ z & 0 & G_s & 0 & 0 \\ x & 0 & 0 & G_s & 0 \\ y & 0 & 0 & 0 & G_s \end{bmatrix}, \quad G_{sh} = \begin{bmatrix} c & z & x & y \\ c & 0 & 0 & 0 & 0 \\ z & 0 & G'_s & 0 & 0 \\ x & 0 & 0 & G'_s & 0 \\ y & 0 & 0 & 0 & G'_s \end{bmatrix} \quad (\text{S.20})$$

where $G_c = A_{NM}/(\rho_{NM}L)$, $G_s = A_{NM}/(\rho_{NM}\lambda_s) \text{csch}(L/\lambda_s)$, and $G'_s = A_{NM}/(\rho_{NM}\lambda_s) \tanh(L/2\lambda_s)$. A_{NM} denotes the NM's area, ρ_{NM} is the NM's resistivity, L is the NM' length, and λ_s is the NM's spin-diffusion length. Similarly, the shunt and series conductance for the FM|NM interface, if the magnet is pointing in the $+\hat{z}$ direction, are defined as:

Eq. (S.21). The new coordinates simplify the system for the purpose of finding the charge to spin conversion ratio, since now the coupled system reduces to the simpler configuration where one magnet (\hat{m}_1) is fixed to the $+\hat{z}'$ direction and injects a spin-current of the form $\vec{I}_s = I_s \hat{z}'$.

Another key point that needs to be considered is *extracting* the component of incident spin currents along the direction of *transmitting* magnets. As such, we need to decompose incident spin currents (such as \vec{I}_{s2} in Fig. S.2) into its constituents. For this purpose, we choose a commonly used non-orthogonal basis for the 2-magnet system [28] ($\hat{m}_1, \hat{m}_2, \hat{m}_1 \times \hat{m}_2$). This allows us to clearly resolve the individual contributions of each magnet to incident spin currents. This new basis can be described by the transformation matrix, A , that turns (z, x, y) to $(\hat{m}_1, \hat{m}_2, \hat{m}_1 \times \hat{m}_2)$:

$$A = \left[\begin{array}{c|ccc} & \hat{m}_1 & \hat{m}_2 & \hat{m}_1 \times \hat{m}_2 \\ \hline z & \cos(\theta_1) & \cos(\theta_2) & \sin(\theta_1) \sin(\theta_2) \sin(\phi_2 - \phi_1) \\ x & \sin(\theta_1) \cos(\phi_1) & \sin(\theta_2) \cos(\phi_2) & \cos(\theta_2) \sin(\theta_1) \sin(\phi_1) - \cos(\theta_1) \sin(\theta_2) \sin(\phi_2) \\ y & \sin(\theta_1) \sin(\phi_1) & \sin(\theta_2) \sin(\phi_2) & \sin(\theta_2) \cos(\theta_1) \cos(\phi_2) - \sin(\theta_1) \cos(\theta_2) \cos(\phi_1) \end{array} \right] \quad (\text{S.23})$$

Then the spin current component of interest is described by:

$$\vec{I}_{s2} = (RA)^{-1} \vec{I}_{s2}(z', x', y') = I_{sm1} \hat{m}'_1 + I_{sm2} \hat{m}'_2 + I_{s\perp} (\hat{m}'_1 \times \hat{m}'_2) \quad (\text{S.24})$$

It may seem that in order to find an analytical expression for \vec{I}_{s2} , we must know (θ_2, ϕ_2) , since the conductance matrices for the second magnet are a function of (θ_2, ϕ_2) . However, the spin current component along the direction of \hat{m}_1 , described by I_{sm1} , is *independent* of the instantaneous direction of \hat{m}_2 . This allows us calculate I_{sm1} , however, in our new coordinate system (where $\hat{m}_1 = \hat{z}'$). The spin-current I_{s2} also needs to be expressed in (z', y', x') .

After these basis transformations and tedious algebra using standard circuit theory, we solve the 2-magnet system and arrive at the analytical expression (keeping only leading order terms for P , since typically $P^2 \ll 1$),

$$\frac{I_{sm1}}{I_c} = \frac{PR_{\text{int}}R_{\text{sp}}}{R_{\text{int}}^2 \text{csch}^2\left(\frac{L_s}{\lambda_s}\right) \sinh\left(\frac{L_{\text{ch}} + 2L_s}{\lambda_s}\right) + 2R_{\text{int}}R_{\text{sp}} \text{csch}\left(\frac{L_s}{\lambda_s}\right) \sinh\left(\frac{L_{\text{ch}} + L_s}{\lambda_s}\right) + R_{\text{sp}}^2 \sinh\left(\frac{L_{\text{ch}}}{\lambda_s}\right)} \quad (\text{S.25})$$

where R_{sp} is defined as the resistance of a block of NM with length λ_s , i.e., $R_{\text{sp}} = \rho\lambda_s/A_{\text{NM}}$ and R_{int} is the interface resistance, $1/G$. L_{ch} and L_s are the side and middle channel lengths of the normal metals (NM).

The total mapping factor for the proposed hardware then becomes $I_M = I_0 (I_c/I_{sm1})$. We used I_M in Fig. 2 to relate our dimensionless Boltzmann models to our full numerical results and have obtained agreement, we also used I_M in Fig. 3 where the interaction strength $J_{12} = I_c/I_M$ was analyzed by sweeping L_{ch} .

It is instructive to consider limits of Eq. (S.25), assuming no spin-relaxation, $\lambda_s \rightarrow \infty$):

$$\frac{I_{sm1}}{I_c} = P \left(\frac{R_{\text{side}}}{R_{\text{int}} + R_{\text{side}}} \right) \left(\frac{R_{\text{side}} \parallel R_{\text{int}}}{2(R_{\text{side}} \parallel R_{\text{int}}) + R_{\text{ch}}} \right) \quad (\text{S.26})$$

where R_{side} and R_{ch} is the charge resistance of the side ($\rho L_s/A_{\text{NM}}$) and middle ($\rho L_{\text{ch}}/A_{\text{NM}}$) channels, respectively.

In our power calculation for significant saturation, we let $I_c = 15I_0 (I_c/I_{sm1})$ to obtain the $I_c^2 R$ dissipation, $R = R_{\text{side}} + R_{\text{int}}$. Pure spin neutral channels can further optimize the power consumption of our proposed device, graphene being a good example [9, 10].

Finally, we add that a special choice of the mixing conductance ($a = 1$) leads to the (θ_2, ϕ_2) independence of I_{sm1} . For arbitrary choices of the mixing conductance, one needs to solve a system of self-consistent equations for every new input I_c such that the (θ_2, ϕ_2) and \vec{I}_{s2} agree.

VII. HEISENBERG AND-GATE: BOLTZMANN APPROACH

This section discusses the definition used to find the reported probabilities for the Heisenberg AND gate by the Boltzmann law. The definition will be discussed for a system of two spins but the same approach was used for the reported AND gate. In Fig. 4, all measurements were taken in the z -direction and continuous spins were binarized by setting $m_{iz} = 0$ as the thresholding point between 0 and 1. Accordingly, to find the probabilities of any logical state using the Boltzmann law, we integrate over the corresponding range for all spins. For example, binarizing two continuous spins produces four states $\{00, 01, 10, 11\}$ and their corresponding probabilities are (states are read as $[m_{1z}, m_{2z}]$):

$$P_{ij} = \int_{\phi_1=0}^{\phi_1=2\pi} \int_{\phi_2=0}^{\phi_2=2\pi} \int_{\theta_1=a}^{\theta_1=b} \int_{\theta_2=c}^{\theta_2=d} \frac{1}{Z} \exp(J_{12} \hat{m}_1 \cdot \hat{m}_2) \sin(\theta_1) \sin(\theta_2) d\theta_1 d\theta_2 d\phi_1 d\phi_2 \quad (\text{S.27})$$

where $i, j \in \{0, 1\}$ and (a, b) or $(c, d) \rightarrow (0, \pi/2)$ when i or j is 1, and (a, b) or $(c, d) \rightarrow (\pi/2, \pi)$ when i or j is 0. For the partition function Z , no special adjustment is required, it is evaluated by doing the normal full integral over the four variables such that the summation of the four probabilities is still equal to one. Similarly, for the Heisenberg AND-Gate the same approach is used to evaluate the probabilities of the $2^3 = 8$ states of the system.

VIII. PROGRAMMING POSITIVE AND NEGATIVE WEIGHTS

To ensure symmetric spin currents incident to all magnets, we inject the same charge current over all LBMs, to create symmetric J_{ij} values. This means however the network can only have all positive or all negative weights. Through graph embedding via auxiliary nodes (Fig. S.3), a mix of positive and negative weights can be obtained, where the role of auxiliary magnets is to have a double negative effect such that $-(-J_{ij}) = +J_{ij}$.

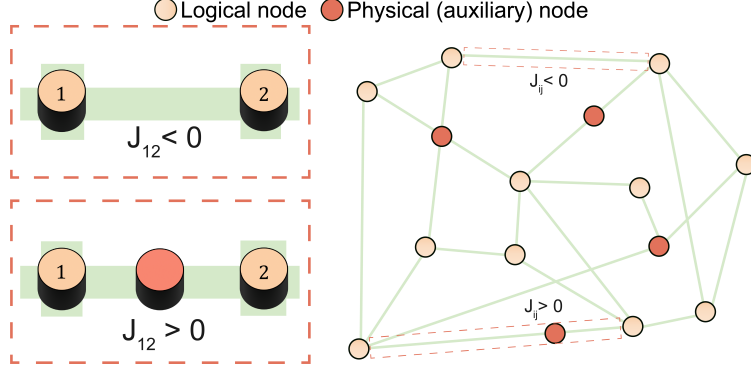


FIG. S.3. Programming \pm weights. Auxiliary magnets are introduced to choose the polarity of the interaction strength J_{ij} , where the input current is fixed such that all magnets have negative correlation ($J_{ij} < 0$). The magnitude of the J_{ij} is tuned by the channel length between any two spins (\hat{m}_i, \hat{m}_j).

IX. PHYSICAL PARAMETERS

Parameter	Value	Unit
Interface polarization (P)	0.1	–
Gilbert damping coefficient (α)	0.01	–
Saturation magnetization (M_s)	1100×10^3	A/m
Magnet volume (Vol.)	$(30 \times 30 \times 2)$	nm^3
Interface conductance (G)	1	S
Spin-Mixing conductance real part (aG)	1	–
Spin-Mixing Conductance Imaginary Part (bG)	0	–
NM Spin-Diffusion Length (λ_s)	400	nm
NM Resistivity (ρ_{NM})	2.35	$\mu\Omega \cdot \text{cm}$
NM Length ($L = L_s = L_{ch}$)	200	nm
NM Area (A_{NM})	1.11×10^{-14}	m^2
Temperature	300	K
Transient Time Step (SPICE)	10	ps

The physical parameters we used in our simulations are reported in the Table above, where the parameters of the NM channel are chosen according to experiments performed in metallic non-local spin valves [31]. The transient noise (.trannoise) function of HSPICE has been used to solve the stochastic differential equations. This solver has been rigorously benchmarked with exact time-dependent Fokker-Planck equations in Ref. [27].